# Complex micelles from the self-assembly of amphiphilic triblock copolymers in selective solvents

**ARTICLE** *in* THE JOURNAL OF CHEMICAL PHYSICS · MAY 2010

Impact Factor: 2.95 · DOI: 10.1063/1.3431203 · Source: PubMed



**5 AUTHORS**, INCLUDING:

Xuejin Li
Brown University
**30** PUBLICATIONS **415** CITATIONS
SEE PROFILE

Mingge Deng
Brown University
**18** PUBLICATIONS **145** CITATIONS
SEE PROFILE

Haojun Liang
University of Science and Technology of Ch…
**152** PUBLICATIONS **2,247** CITATIONS
SEE PROFILE

# Complex micelles from the self-assembly of coil-rod-coil amphiphilic triblock copolymers in selective solvents

**Pengtao He,[ab] Xuejin Li,*[ab] Mingge Deng,[ab] Tao Chen[ab] and Haojun Liang*[ab]**

***Received 15th December 2009, Accepted 11th January 2010***
***First published as an Advance Article on the web 11th February 2010***
**DOI: 10.1039/b926370e**

We report an extensive simulation study on the spontaneous formation of complex micelles from coil-rod-coil amphiphilic triblock copolymers in dilute solution resulting from solvent selectivity. The amphiphilic molecule is built from one hydrophilic block on each side and a hydrophobic block in the middle. The rigidity of the rod block is introduced by adding a bond-bending potential of the angle among three subsequent particles in the hydrophobic block. The incorporation of rigid-rod block into the amphiphilic block copolymer results in the self-assembled microstructures and their corresponding properties that differ from those built from fully flexible amphiphilic molecules with the same conditions. By changing the selectivity of solvents, defined in terms of the repulsive interactions between the solvent and the hydrophilic/hydrophobic particles, we find that the aggregation morphology changes from bundle-like micelles to spherical and cylindrical micelles to elongated micelles and then to ring-like toroidal micelles, revealing that the selectivity of solvents is a key factor that determines aggregation morphology. In addition, we observe that the formation of toroidal micelles from coil-rod-coil amphiphilic triblock copolymers proceeds *via* the growth pathway, which is quite distinct from the conventional toroidal micelle coalescence pathway observed in the self-assembling process of fully flexible amphiphilic triblock copolymer systems. Chain packing in toroidal micelles formed from amphiphilic triblock copolymers with fully flexible hydrophobic and rigid-rod hydrophobic blocks is likewise investigated. The simulation results show that the rigid-rod middle blocks adopt only extended conformations while flexible-coil middle blocks can adopt both folded and extended conformations in toroidal micelles. These findings demonstrate that the bond-bending potential in amphiphilic molecules is an effective and relatively simple method to model the behavior of coil-rod-coil amphiphilic block copolymers.

## 1. Introduction

Amphiphilic block copolymers in selective solution self-assemble into a variety of morphologies, such as spherical and cylindrical micelles, bilayers, vesicles, and nanotubes.[1,2] Compared to small molecular weight amphiphiles, aggregates from amphiphilic block copolymers are more thermodynamically and kinetically stable. Aggregates of block copolymers in selective solution thus have the potential to be used in a broad range of applications, especially in the fields of drug delivery, microelectronics, and advanced materials.[3,4] The block copolymers investigated for these applications generally have flexible-coil blocks due to the flexibility of their polymer chains. The self-assembly behaviors and aggregate structures of amphiphilic block copolymers with flexible chains in two or three blocks have been a topic of high importance in the past decade,[5–8] and the current understanding about the phase behaviors of many amphiphilic block copolymers is largely based on these systems. It is generally believed that three factors, core-chain stretching entropy, interfacial energy, and intercoronal chain interaction, determine the micellization of coil-coil amphiphilic block copolymers.

Recently, more attention has been given to rod-coil amphiphilic block copolymers composed of rigid-rod blocks bonded to flexible-coil blocks. Besides the chemical composition, the existence of an anisotropic orientation of rigid-rod blocks, the effect of chain topology on conformational entropy, and molecular packing geometries also show profound influence on the self-assembly of the block copolymers. As such, the self-assembly of rod-coil block copolymers is fundamentally different from that of classical coil-coil amphiphilic block copolymers. Based on the functionality of the rigid-rod blocks, there is growing interest in amphiphilic block copolymers with rod-coil structures, and a number of intriguing phases, including wavy lamellae, zigzags, arrowheads, straight lamellae, perforated lamellae, hexagonal strips, honeycombs, and hollow spherical micelles, have been observed through self-assembly from them.[9–18] The ability of rod-coil amphiphilic block copolymers to form rich and complex self-assembled structures has been clearly demonstrated in experimental studies by Chen *et al.*[9,10] Specifically, they observed a variety of fascinating structures that had not been previously observed in coil-coil amphiphilic block copolymers, including arrowheads, wavy lamellae, and zigzag lamellae, from the self-assembly of PHIC-*b*-PS rod-coil amphiphilic block copolymers.

[a]*CAS Key Laboratory of Soft Matter Chemistry, Department of Polymer Science and Engineering, University of Science and Technology of China, Hefei, Anhui, 230026, People's Republic of China. E-mail: xjli7@ustc.edu.cn; hjliang@ustc.edu.cn*
[b]*Hefei National Laboratory for Physical Sciences at Microscale, University of Science and Technology of China, Hefei, Anhui, 230026, People's Republic of China*

Further studies on the PHIC-*b*-PS system confirm that the kinetics formation of these structures depend strongly on the selectivity of solvents.[11,12] Jenekhe and Chen studied the self-assembled aggregates of PPQ-*b*-PS rod-coil amphiphilic block copolymers in solution.[13,14] The morphologies of hollow spherical, cylindrical, vesicular, and lamellar aggregates were observed by changing solvent composition. Mao and Turner investigated the solution properties of rigid polyampholyte-based rod-coil amphiphilic block copolymers.[15] They found that chain rigidity revealed a dramatic effect on the electrostatic interactions between polyelectrolytes, which exhibited intriguing differences from flexible ones.[16] Microphase separation and the formation of complex micelles were also studied in coil-rod-coil amphiphilic triblock copolymers.[17,18] Besides these extensive experimental investigations, a number of theoretical models have been developed to understand the self-assembly behavior of rod-coil amphiphilic block copolymers.[19–30] Here, we briefly describe a few of the major achievements. A precursory work was presented by Semenov and Vasilenko,[19] who studied the lamellar to nematic transition of rod-coil block copolymers using analytical theory. Williams and Fredrickson proposed the hockey puck micelle where the rods are packed axially into cylinders covered by coils.[20] They predicted that the hockey puck structure would be stable at large coil fractions. Holyst and Schick calculated the phase behavior of rod-coil block copolymers in the weak segregation and weak alignment limit using the Landau Theory.[21] Reenders and Brinke derived the Landau free energy function and expanded the density order up to four-order to understand the phase behavior of rod-coil block copolymers.[22] The self-consistent field theory (SCFT) method was also applied to rod-coil block copolymer systems. Matsen and Barett performed SCFT simulations of rod-coil block copolymers in the Semenov model.[23] Pryamitsyn and Ganesan applied similar SCFT calculations with the Maier-Saupe type rod-rod aligning interactions and explored the phase diagram for rod-coil block copolymer for one and two dimensions.[24] Some theoretical models do not consider aligning interactions between the rods. For instance, Li and Gersappe studied the phase diagram of rod-coil block copolymer by proposing a two-dimensional SCFT lattice-based model where the chain rigidity was accounted for by the rotational isomeric state scheme.[25] In addition, the self-assembly behavior of linear and T-shaped rod-coil block copolymers melted by applying a three-dimensional SCFT lattice-based model was studied by An *et al.*[26–29] In a series of recent studies, Sullivan *et al.*[30–32] simulated the phase behavior of rod-coil block copolymers using SCFT with the wormlike chain model. They adopted a hybrid approach to numerically solve the diffusion equations of the propagator for wormlike chains and obtained some ordered phases with axial symmetries, such as the nematic and smectic-A phases. These theoretical studies help researchers better understand both ordered structures and ordering transition.

In addition to these theoretical studies, particle-based mesoscopic simulation studies on the self-assembly behavior of rod-coil block copolymers have also been performed by a few groups using various computer techniques, such as Brownian dynamics,[33–37] dissipative particle dynamics,[38] and Monte Carlo simulations.[39,40] However, most of them focus on the liquid-crystalline behavior of rod-coil block copolymer systems and papers on the computer simulation of solution-state self-assembly of rod-coil block copolymers are seldom reported. Glotzer and co-workers developed a generic model of tethered nano building blocks to simulate amphiphilic block copolymers and surfactants microphase separation and liquid-crystal phase ordering using the Brownian dynamics method.[41–46] They predicted a variety of fascinating microstructures, including sheets, wires, tubes, honeycombs, helical scrolls, and alternating cylinders, from the self-assembly of rod-coil amphiphilic block copolymers in solutions. Song *et al.* applied lattice Monte Carlo simulation to study the phase behavior of symmetric ABA-type triblock copolymers.[47] Despite these previous studies, a more fundamental study on the self-assembled microstructures of rod-coil block copolymers depending on the selectivity of solvents and the acquisition of a good understanding of the detailed relationship between the self-assembled microstructures and molecular parameters remain very challenging tasks.

In this paper, the self-assembled microstructures of coil-rod-coil ABA-type amphiphilic triblock copolymers, depending on the selectivity of solvents for each block, are studied using a dissipative particle dynamics (DPD) approach. Specifically, this work focuses on how rigid-rod hydrophobic blocks affect aggregations of the microstructures and the dynamic properties of amphiphilic block copolymers in selective solvents. In our previous simulations, we have successfully applied the DPD method to investigate the dynamic self-assembly of complex micelles from fully flexible amphiphilic triblock copolymers in selective solvents.[48,49] In order to consider the rigidity of a rod block, a bond-bending potential of the angle is introduced to the amphiphilic triblock copolymer system, that is, a bond-bending force among three subsequent particles in the hydrophobic block is considered in the DPD model. In previous simulations, the introduced bond-bending potential has been successfully applied to model the chain rigidity of homopolymers[50] and block copolymers.[47,51] Rigid molecules have also been simulated with DPD.[52–56] The influence of the chain rigidity on the nanostructures of miktoarm block copolymers was investigated by Qian *et al.*[54,55] In their study, a typical spherical ordered structure was obtained for a coil-coil miktoarm block copolymer in melt. By introducing a bond angle potential, lamellar structures were formed. Thus, the existence of constrained bond angles makes it possible to realize the bending rigidity, and the modified DPD method may be applicable for studying the self-assembly behavior of coil-rod-coil amphiphilic triblock copolymers in selective solvents.

## 2. Model and method

### 2.1 Mesoscopic model for coil-rod-coil amphiphilic triblock copolymers

We adopt the dissipative particle dynamics simulation method to study the self-assembly behavior of a mesoscopic model for coil-rod-coil amphiphilic triblock copolymers. Within the DPD approach, the amphiphilic molecule in our study is represented by a coarse-grained model with hydrophilic and hydrophobic blocks. In order to provide parameters that are comparable to classical amphiphilic triblock copolymers, the model is derived from the mesoscopic model for fully flexible amphiphilic triblock

 

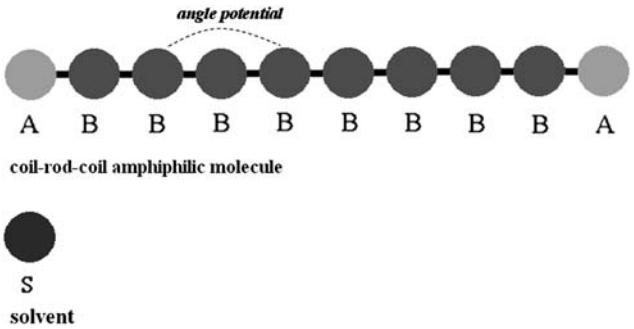


**Fig. 1** Schematic representation of the simulation model of coil-rod-coil amphiphilic molecule. In the figure, Particle A is hydrophilic, while Particle B is hydrophobic. Particle S represents the solvent, which is not shown in the figures.

copolymers[48] and is extended to account for the presence of an extra bond-bending potential between the consecutive bonds of rigid-rod blocks. Specifically, this model is built with one hydrophilic particle on each side and eight hydrophobic particles in the middle, that is, an amphiphilic $A_1B_8A_1$ triblock copolymer molecule is modeled, in which Particle A is hydrophilic and Particle B is hydrophobic. Particles A and B particles are also referred to as *soluble* and *insoluble* blocks, respectively. To present the chain rigidity of amphiphilic molecule, the connections among the three consecutive hydrophobic particles are constrained to a certain angle, as shown in Fig. 1. The coil block is modelled as one particle, which is considered to be, perhaps, too simple to represent the characteristic of the coil block. In our simulations, however, few constraints imposed on the bond-bending potential of the angle among the side Particle A and two consecutive Particles B make it possible to describe the effect of the coil block structure on the self-assembly of coil-rod-coil amphiphilic triblock copolymers. In previous particle-based simulations, $A_1B_n$- and $A_1B_nA_1$-type amphiphilic molecules have been successfully applied to study the self-assembly behavior and microphase separation of coil-coil block copolymer.[52,57–61] In addition, as mentioned earlier, the influence of chain rigidity on the nanostructures of the $A_2(B_n)_2$-type miktoarm block copolymers has been investigated using the DPD simulation technique by Qian *et al.*[54] The simple model of an amphiphilic molecule built with one hydrophilic particle on each side is considered to be appropriate for simulating the characteristics of coil-rod-coil amphiphilic molecules. To simulate amphiphilic molecules in a selective solution, the solvent is included explicitly in the simulation and is modeled as a single particle (denoted by S). For clarity, however, solvent particles are not shown in the figures. Moreover, the density of the hydrophobic particles is measured, allowing us to investigate the formation process in detail. In the rich domains of hydrophobic particles, the density is high, whereas in the rich domains of hydrophilic/solvent particles, it is low (or reduced to zero).

### 2.2 Dissipative particle dynamics formulation

We study the self-assembly of coil-rod-coil amphiphilic triblock copolymers with the help of the DPD simulation technique. DPD is a simple but intrinsically promising simulation method that allows the study of the phase behaviors of block copolymers. In DPD simulation, a particle represents the center of mass in a cluster of atoms, and the position and momentum of the particle is updated in a continuous phase but spaced at discrete time steps. Particles i and j at positions $r_i$ and $r_j$ interact with each other *via* pairwise conservative, dissipative, and random forces, which are given by:

$$\mathbf{F}^{C}_{ij} = a_{ij}\omega(r_{ij})\mathbf{n}_{ij} \tag{1}$$

$$\mathbf{F}^{D}_{ij} = -\gamma\omega^2(r_{ij})(\mathbf{n}_{ij}\cdot\mathbf{v}_{ij})\mathbf{n}_{ij} \tag{2}$$

$$\mathbf{F}^{R}_{ij} = \sigma\omega(r_{ij})\zeta_{ij}\Delta t^{-1/2}\mathbf{n}_{ij} \tag{3}$$

where $\mathbf{r}_{ij} = \mathbf{r}_i - \mathbf{r}_j$, $r_{ij} = |\mathbf{r}_{ij}|$, $\mathbf{n}_{ij} = \mathbf{r}_{ij}/r_{ij}$, and $\mathbf{v}_{ij} = \mathbf{v}_i - \mathbf{v}_j$. The parameter $a_{ij}$ is the repulsion strength, and $\sigma$ and $\gamma$ are the noise and friction parameters coupled by $\sigma^2 = 2\gamma k_B T$. $\zeta_{ij}$ is a Gaussian white, which is characterized by a zero mean and unit variance:

$$\langle\zeta_{ij}(t)\rangle = 0 \tag{4}$$

$$\langle\zeta_{ij}(t)\zeta_{kl}(\tau)\rangle = (\delta_{ik}\delta_{jl} + \delta_{il}\delta_{jk})\delta(t-\tau) \tag{5}$$

The weight function $\omega(r_{ij})$ is given by:

$$\omega(r_{ij}) = \begin{cases} 1 - r_{ij}/r_c & r_{ij} < r_c \\ 0 & r_{ij} \geq r_c \end{cases} \tag{6}$$

where $r_c$ is the cutoff radius, which gives the extent of interaction range. In the present simulations, we have chosen the cutoff radius of interaction and the particle mass to be all equal to unity, hence $r_c = m = 1.0$. The total force can also have an elastic contribution, which is derived from the harmonic force used to connect two consecutive particles in the chains of polymers.[62] This contribution is expressed as:

$$\mathbf{F}^{s}_{ij} = k_s(1 - r_{ij}/r_s)\mathbf{n}_{ij} \tag{7}$$

where $k_s$ and $r_s$ are the spring constant and equilibrium bond length between two consecutive particles, respectively. To control the chain flexibility, an extra bond-bending force between consecutive bonds in hydrophobic section is also added

$$\mathbf{F}^{\theta} = -\nabla V_{\text{bend}} \tag{8}$$

$$V_{\text{bend}} = \tfrac{1}{2}k_\theta(\theta - \theta_0)^2 \tag{9}$$

where $k_\theta$ and $\theta_0$ are the bending constant and the equilibrium angle between two consecutive bonds, respectively.

The dynamics of the DPD particles are followed by solving Newton's equation of motion with the forces above using a modified version of velocity-Verlet algorithm:

$$\begin{aligned} \mathbf{r}_i(t+\delta t) &= \mathbf{r}_i(t) + \mathbf{v}_i\delta t + \frac{1}{2}\mathbf{f}_i(t)\delta t^2 \\ \tilde{\mathbf{v}}_i(t+\delta t) &= \tilde{\mathbf{v}}_i(t) + \lambda\mathbf{f}_i(t)\delta t \\ \mathbf{f}_i(t+\delta t) &= \mathbf{f}_i\big(\mathbf{r}_i(t+\delta t),\ \tilde{\mathbf{v}}_i(t+\delta t)\big) \\ \mathbf{v}_i(t+\delta t) &= \mathbf{v}_i(t) + \frac{1}{2}\big(\mathbf{f}_i(t) + \mathbf{f}_i(t+\delta t)\big)\delta t \end{aligned} \tag{10}$$

where $\mathbf{f}_i$ is the total force on a particle $i$ and $\tilde{\mathbf{v}}_i$ denotes a predicted velocity which is corrected in the last step of the algorithm.

### 2.3 Simulation condition

The total of 192 000 particles is used in the simulation at a particle density of 3 in a cubic box of size 40 $r_c \times 40$ $r_c \times 40$ $r_c$with periodic boundary conditions. The total number of constituent particles of amphiphilic molecules is set at 9 600; therefore, the concentration of the amphiphile is 5.0 vol%. The simulations are initiated by placing the coil-rod-coil $A_1B_8A_1$ amphiphilic triblock copolymers at random in the cubic box, followed by equilibration with all the repulsion parameters set to the same value, $a_{ii} = 25.0$. This results in a highly disordered and mixed system. The rod-coil repulsive parameter, which is related to the interaction between Particles A and B, is then increased to $a_{AB} = 50.0$. After these parameters are selected, the microstructure of the coil-rod-coil amphiphilic triblock copolymer can be solely determined by the selectivity of solvents (*i.e.*, the interactions between the Solvent and the Particles A/B). To model the amphiphilic nature of triblock copolymers, the repulsion parameter between the hydrophilic (A) and solvent (S) particles is made smaller than the repulsion parameter between two like particles. Likewise, the parameter related to the interaction between the hydrophobic (B) and solvent (S) particles is made larger than the repulsion parameter between two similar particles, which ensures that the hydrophobic block of amphiphile is sufficiently shielded from the solvents.

Regarding the elastic contribution to the interaction energy, the spring constant is given by $k_s = 4.0$ and the equilibrium bond length $r_s = 0.86\ r_c$. The hydrophobic part of amphiphilic molecules is considered fairly rigid in our study; therefore the value of the equilibrium angle in the rigid blocks is set to $\theta_0 = 180°$. To determine the bending constant, $k_\theta$, for the amphiphilic molecules, we require that the angular distribution of rigid blocks be within our statistical accuracy. A value of $k_\theta = 10.0$ is found to satisfy this requirement. The simulations are performed using a modified version of the DPD code named MYDPD.[63] The DPD friction parameter $\gamma$ is set to 4.5 in our study. Time integration of motion equations is calculated by the modified velocity–Verlet algorithm with $\lambda = 0.65$ and time step $\Delta t = 0.03$.

## 3. Results and discussion

In this section, we present the results from simulations of coil-rod-coil $A_1B_8A_1$ amphiphilic triblock copolymer systems.

Depending on the selectivity of solvents, defined in terms of the repulsive interactions between Solvent and Particles A/B, amphiphilic triblock copolymers have the capacity to self-assemble into a variety of complex microstructures, such as spherical micelles, Y-like junctions, toroidal micelles, oblate micelles, and vesicles, which have been observed in our early simulations.[48,49] Along with the introduction of an extra bond-bending force between the consecutive bonds of the hydrophobic section to the amphiphilic system, the hydrophobic block transforms from a fully flexible segment into a fairly rigid one, while the phases and corresponding properties are anticipated to change significantly. To illustrate the effects of the selectivity of solvent of amphiphilic molecules on microstructure formation,

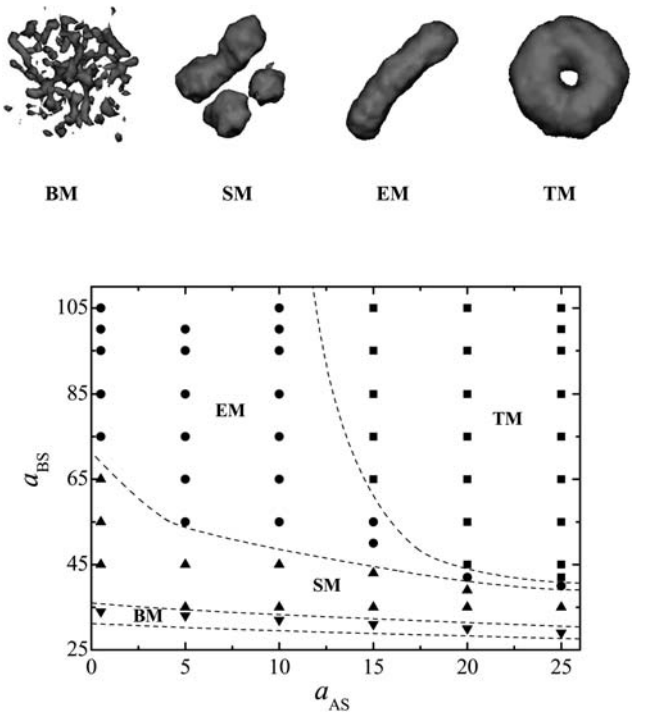


**Fig. 2** Phase diagram of the coil-rod-coil amphiphilic triblock copolymer system in selective solution for a range of repulsive parameters $a_{AS}$ and $a_{BS}$. The microstructures included: (i) bundle-like micelles (BM); (ii) mixtures of spherical and cylindrical micelles (SM); (iii) elongated micelles (EM); and (iv) ring-like toroidal micelles (TM). The dashed lines in the figure serve as visual guides.

we systematically vary these two repulsive parameters and examine the modulated microstructures for a series of systems. Fig. 2 shows coil-rod-coil amphiphilic molecules self-assembled into a series of complex microstructures, including bundle-like micelles, spherical micelles, cylindrical micelles, elongated micelles and ring-like toroidal micelles, which are different from those produced by fully flexible amphiphilic molecules in the same conditions. In our simulations, we have not observed lamellar and hockey puck micelles. As predicted by previous studies, the hockey puck micelles would be stable at large coil fractions,[20] while lamellar micelles preferred at high concentration of amphiphilic molecules with symmetric or quasi-symmetrical block copolymers.[27] In this study, we pay our attention to the influence of solvent selectivity to the self-assembled microstructures of coil-rod-coil amphiphilic triblock copolymers at a low coil volume fraction of approximately 0.25 and a low concentration of amphiphilic molecules of 5.0 vol%. In our opinion, the lamellar and hockey puck micelles could be obtained if the coil fraction and concentration of amphiphilic molecules were increased to higher values.

In our earlier studies, we note that the geometric shapes packed with fully flexible triblock copolymers can be described in terms of shape factor.[49] When an extra bond-bending potential is introduced to the amphiphilic system, however, the rigidity of the rod block leads to the maintenance of an approximately constant length of long hydrophobic blocks. The normalized distribution of end-to-end distance for amphiphilic molecules built from fully flexible hydrophobic and rigid hydrophobic blocks with the same

 

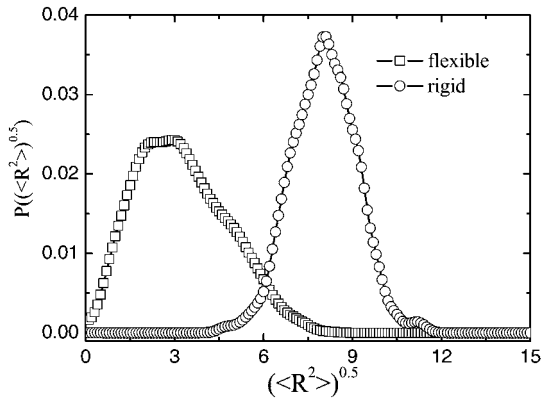


**Fig. 3** Distribution of end-to-end distance for amphiphilic triblock copolymers built with fully flexible hydrophobic and fairly rigid hydrophobic blocks.

DPD repulsive interactions is plotted in Fig. 3. In the case of fully flexible chains, a broad peak distribution is observed, and the values of the main peak are distributed in the range from 1.9 $r_c$ to 3.0 $r_c$. For fairly rigid chains, the distribution of end-to-end distance turns into a sharp one and the peak shifts toward a value of $\sim$8.0 $r_c$, which is higher than that of fully flexible chains. It is clear that the existence of an extra bond-bending force leads to the increase in individual chain sizes, owing to the rigidity of the hydrophobic block. Thus, the shape factor is not currently suitable to predict the geometric shapes packed by rigid chains.

Next, we consider the perpendicular line corresponding to $a_{AS} = 15.0$ in the phase diagram, a case for mediating hydrophilic short blocks. In the areas of $a_{BS} = 29.0\sim33.0$ in the phase diagram (Fig. 2), the coil-rod-coil amphiphilic triblock copolymers are no longer aggregated into spherical micelles. Instead, they form a variety of bundle-like micelles in order to avoid the intimate connections between rigid-rod hydrophobic sections and solvent particles. The long rigid-rod blocks of coil-rod-coil amphiphilic triblock copolymers in the bundle-like micelles align with each other, and the direction of these blocks tends to be perpendicular to the radial direction of bundle-like micelles. The molecular packing observed is similar to the wire-like micelle formed by T-shaped graft copolymers with rigid backbones.[33] As $a_{BS}$ is increased to 45.0, the bundle-like micelles gradually aggregate with each other in order to reduce the rigid-rod hydrophobic interaction energy, while spherical micelles appear. The direction of the rigid-rod blocks is approximately parallel to the radial direction of the micelles. The rigidity of the long hydrophobic blocks makes it easier for two neighboring hydrophobic sections to keep in contact with each other and form a complex cylindrical micelle; the intra-association sections of the complex cylindrical micelle can induce a drastic increase in bond-bending energy, thus making the aggregates unstable. The system then adopts a strategy to reduce this energy, that is, the complex cylindrical micelle can realign to form an elongated micelle at $a_{BS} = 45.0\sim62.0$. Further increases in $a_{BS}$ cause the formation of ring-like toroidal micelle.

To develop the skills necessary to control the sizes and shapes of self-assembled micelles, detailed dynamic information regarding the process of spontaneous micelle formation under different conditions is required. However, this process generally occurs too rapidly to be captured *via* present experimental measurements. Hence, the simulation provides a good method to understand this process. Theoretical studies and experimental observations have suggested that the formation of toroidal micelles can proceed *via* either a conventional micelle coalescence pathway[7,64] or a growth pathway.[65,66] In our previous simulations, we observed that some microstructures of complex morphology include toroidal micelles resulting from fully flexible triblock copolymers in selective solvents.[48] We also found that the dynamic process of toroidal micelle formation is in agreement with the phenomenological description of the conventional micelle coalescence pathway. This process first starts with the formation of small spherical and cylindrical micelles, followed by their aggregation, giving rise to Y-like junctions. From these, toroidal micelles are finally formed. Similarly, the dynamic processes involved in the formation of complex microstructures from coil-rod-coil amphiphilic triblock copolymers can be easily observed by employing the DPD method. Fig. 4 shows a similar pathway of spontaneous toroidal micelle formation from coil-rod-coil $A_1B_8A_1$ amphiphilic triblock copolymers in the case of intermediate hydrophilicity of Block A ($a_{AS} = 15.0$). It reveals that the amphiphilic molecules initially aggregate rapidly into bundle-like micelles (Fig. 4a–4b). The bundle-like micelles then come into close contact with each other and form a complex cylindrical structure (Fig. 4c). The complex cylindrical structure

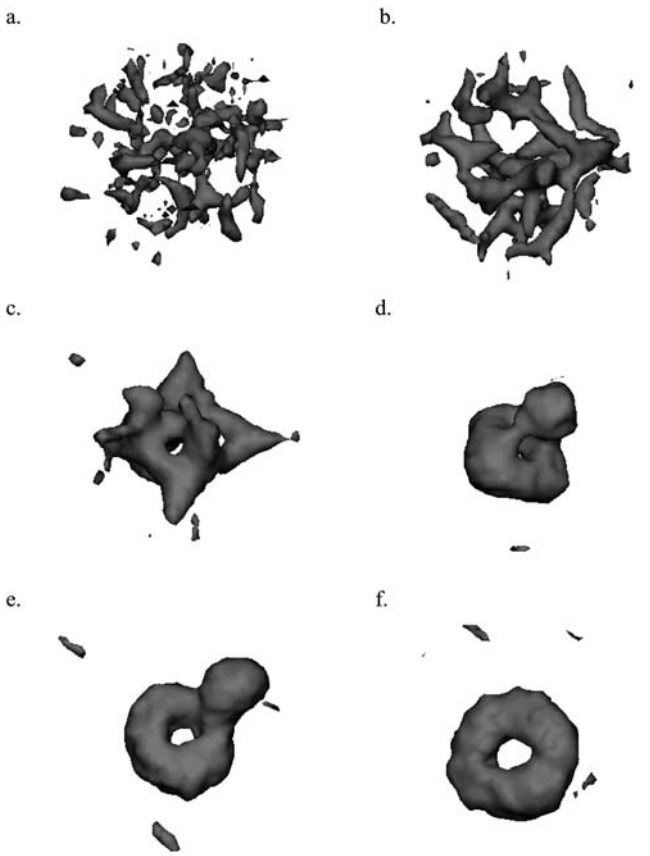


**Fig. 4** Sequential snapshots of the formation of toroidal micelle from coil-rod-coil amphiphilic triblock copolymers in selective solution for $a_{AS} = 15.0$ and $a_{BS} = 75.0$ at $t =$ (a) 1000, (b) 3000, (c) 6000, (d) 15000, (e) 30000, and (f) 95000.

subsequently evolves into a toroidal micelle with one end-cap (Fig. 4d–4e). A closed ring-like toroidal micelle is finally formed when the end-cap merges into the micelle (Fig. 4f).

When the value $a_{AS}$ is increased ($a_{AS} = 25.0$), an alternate pathway, which is in agreement with the phenomenological description of the growth pathway for the formation of toroidal micelle, is observed, as shown in Fig. 5. In this process, the coil-rod-coil $A_1B_8A_1$ amphiphilic triblock copolymers still begin to aggregate into bundle-like micelles (Fig. 5a–5b). The bundle-like micelles then rapidly encapsulate water particles and form a disk-like vesicle (Fig. 5c–5d). However, this disk-like vesicle is unstable. It pinches off at the center and transforms into a toroidal structure with a single hole (a torus) (Fig. 5e–5f). This pathway for the formation of pure ring-like toroidal micelles from vesicles is similar to the growth pathway that is observed for micelles assembling into a rod, to a vesicle, and then to a ring structure. However, we have not observed this pathway in the self-assembly process of toroidal micelles from fully flexible triblock copolymer systems.

Our results suggest that bundle-like micelles can form spontaneously through the clustering of rigid-rod segments, owning to the amphiphilic nature of the amphiphilic triblock copolymers and the rigidity of rod blocks. The system then adopts different strategies for the different hydrophilicities of short blocks. The bundle-like micelles come into contact with each other to form complex cylindrical micelles, which gradually evolve into toroidal micelles. With the decrease in the hydrophilicity of short blocks, the bundle-like micelles can encapsulate solvent particles to form disk-like vesicles. These disk-like vesicles, however, are unstable and transform into toroidal micelles spontaneously.

It is interesting to investigate micelle structures and chain packing in the self-assembly of coil-rod-coil amphiphilic triblock copolymers in selective solvents. In order to provide a more quantitative insight into the characteristics of the ring-like toroidal micelles produced from coil-rod-coil amphiphilic triblock copolymers, we calculate the variation of the densities of each segment with the distance from the center of mass of the micelle, as shown in Fig. 6a. We note that the Solvent is present both inside and outside the micelles. Two peaks for the curve of Segment A correspond to the densities of Segment A at the outer and inner surface of the ring-like toroidal micelle, respectively. From the distance between the two peaks, it can be determined that the thickness of the toroidal micelle is $\sim 9.6\ r_c$. For comparison, the variation of the densities as a function of the radii around the mass center of toroidal micelle from fully flexible amphiphilic triblock copolymers is also calculated, as shown in Fig. 6b. From this figure, we obtained a micelle thickness of $\sim 8.4\ r_c$. The simulation results indicate that the thickness of the pure ring-like toroidal micelle from coil-rod-coil amphiphilic

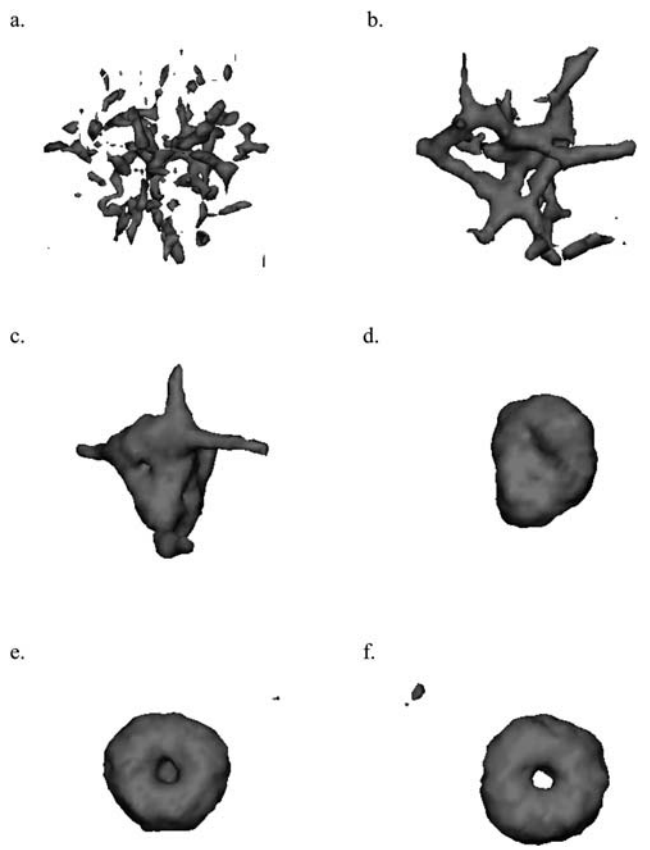


**Fig. 5** Sequential snapshots of the formation of toroidal micelle from coil-rod-coil amphiphilic triblock copolymers in selective solution for $a_{AS} = 25.0$ and $a_{BS} = 75.0$ at $t =$ (a) 1000, (b) 3000, (c) 6000, (d) 15000, (e) 40000, and (f) 45000.

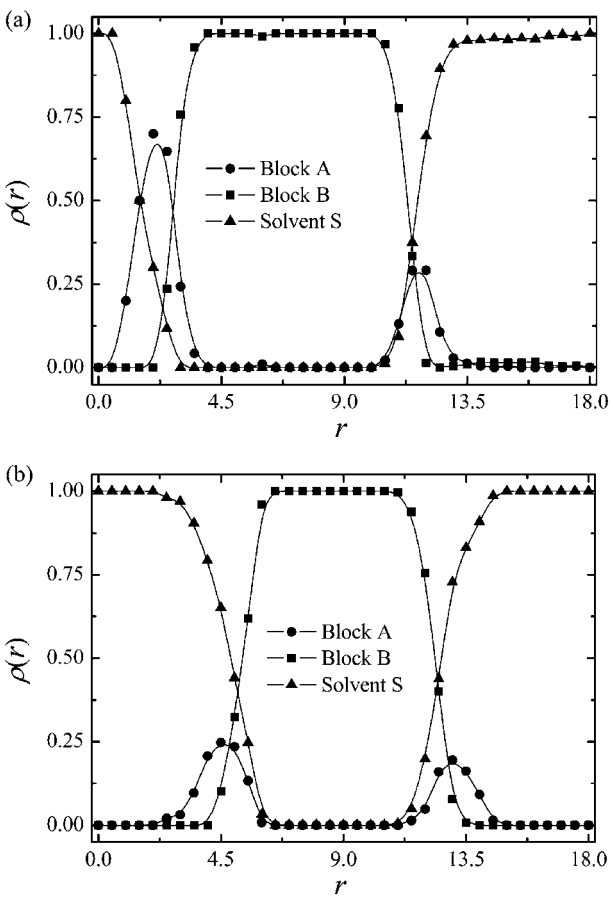


**Fig. 6** The variation of the densities of Block A, Block B, and Solvent S particles with $r$ in pure ring-like toroidal micelles from amphiphilic triblock copolymers built with (a) fairly rigid hydrophobic and (b) fully flexible hydrophobic blocks. $r$ is the radius around the mass center of the pure ring-like toroidal micelle.

triblock copolymers is larger than that of micelles from fully flexible amphiphilic triblock copolymers. Moreover, the inner radius of the circular hole in the pure ring-like toroidal micelle can be obtained from the distance from the center of mass of the micelle to the peak of its inner surface. The corresponding values of the radius for amphiphilic molecules with fully flexible hydrophobic and fairly rigid hydrophobic blocks are $\sim$4.4 $r_c$and $\sim$2.1 $r_c$, respectively. We notice that the radius of the pure ring-like toroidal micelle from coil-rod-coil triblock copolymers is obviously smaller than that from fully flexible amphiphilic triblock copolymers. One possible reason for this may have to do with liquid crystalline defects for packing rigid-rod blocks in a coil-rod-coil amphiphilic triblock copolymer system. The polymer chains in coil-rod-coil amphiphilic triblock copolymers tend to increase occupied interfacial area thereby minimizing the liquid crystalline bending energy.

To gain insights into the packing of polymer chains in the micelles, we calculate the angle, $\varphi$, between the vectors from the center of mass of middle Block B to the centers of mass of each Block A, and investigate the angular distribution, $P(\varphi)$, in pure ring-like toroidal micelles from amphiphilic triblock copolymers built from fully flexible hydrophobic and fairly rigid hydrophobic blocks with the same DPD repulsive interactions. It had been previously proposed that the following equation is used to calculate the cos$\varphi$,[67]

$$\cos\phi = \frac{(\mathbf{r}_{A1} - \mathbf{r}_B)\cdot(\mathbf{r}_{A2} - \mathbf{r}_B)}{|\mathbf{r}_{A1} - \mathbf{r}_B||\mathbf{r}_{A2} - \mathbf{r}_B|} \quad (11)$$

where $\mathbf{r}_{A1}$, $\mathbf{r}_B$, and $\mathbf{r}_{A2}$ are the position vectors of the centers of mass of the first side Block A, the middle Block B, and the second side Block A, respectively. For convenience, we use the terms "folded chain" and "extended chain" to describe chain conformation. The folded chain can be briefly estimated from the angle $\varphi$. If the angle is smaller than 90°, the chain is called a folded chain. Otherwise, it is called an extended chain. Fig. 7 shows two representative results of $P(\varphi)$ for polymer chains in the pure ring-like toroidal micelle. In the case of amphiphilic molecules with fully flexible hydrophobic blocks, we find that the angle can take a wide variety of values, which implies that both folded and extended chains dominate chain conformation in the ring-like toroidal micelle. The existing broad distribution of angles can be explained by the flexibility present in the amphiphilic molecular backbone. For fully flexible block copolymers, the polymers have Gaussian coil chain shapes and satisfy random walk statistics. In theory, it is possible for the angle to take on any value. However, in the case of amphiphilic molecules with rod blocks, the distribution shows an obvious increase at $\varphi > 105°$ and a peak near $\varphi = 160°$, indicating that there hardly exist any folded chains in the corresponding micelle. As we know, the lack of chain flexibility in rod-coil block copolymer systems leads to an extended rigid chain conformation, and the packing of the rigid blocks creates liquid crystalline defects, resulting in a parallel alignment between the particles of two rod B blocks. In our simulations, the rod block is large relative to the coil block and the probability having a smaller angle becomes very low.

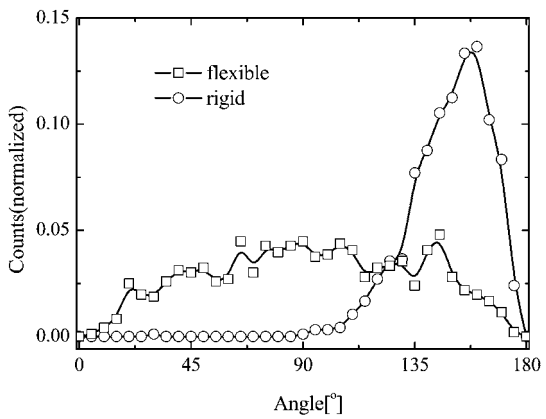


**Fig. 7** Normalized distribution of $P(\varphi)$ for chains in pure ring-like toroidal micelles from amphiphilic triblock copolymers with fully flexible hydrophobic and fairly rigid hydrophobic blocks, where $\varphi$ is the angle between the vectors from the center of mass of the middle rod Block B to the centers of mass of each Block A.

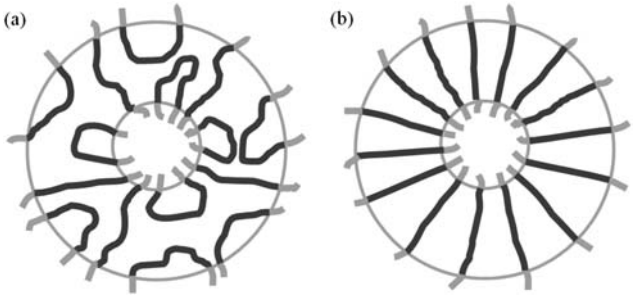


**Fig. 8** Schematic diagrams showing the chain packing in pure ring-like toroidal micelles from amphiphilic triblock copolymers built with (a) fully flexible hydrophobic and (b) fairly rigid hydrophobic blocks in selective solutions.

On the basis of the simulation results discussed above, we obtain the schematic chain packing in the representative micelles, as illustrated in Fig. 8. In the pure ring-like toroidal micelle, the hydrophilic blocks pack on the outside of the micelle, while the hydrophobic blocks constitute the micelle wall. For fully flexibly amphiphilic triblock copolymers, both folded and extended chain conformations dominate chain conformation in the micelle. For coil-rod-coil amphiphilic triblock copolymers, favorable rod alignment and molecular rigidity result in extended chain conformations.

## 4. Conclusions

In this paper, we studied the microstructures assembled from coil-rod-coil amphiphilic triblock copolymers in selective solvents using the dissipative particle dynamics (DPD) approach. The DPD model of an amphiphilic molecule had one hydrophilic block on each side and a hydrophobic block in the middle. The chain rigidity of the rod block was introduced by an extra bond-bending potential of the angle. The coil-rod-coil amphiphilic molecules can self-assemble into complex microstructures, such as bundle-like micelles, spherical micelles, cylindrical micelles, elongated micelles and toroidal structures, which are different from those built from fully flexible amphiphilic molecules in the same conditions. Two different pathways in the formation of pure ring-like toroidal micelles were observed in our simulations. Interestingly, the formation of toroidal micelle from coil-rod-coil triblock copolymers proceeded *via* the growth pathway, which is

quite distinct from the conventional toroidal micelle coalescence pathway observed in the self-assembly process from fully flexible amphiphilic triblock copolymer systems. Moreover, chain packing in toroidal micelles from amphiphilic triblock copolymers built with fully flexible hydrophobic and fairly rigid hydrophobic blocks was investigated. It was observed that the rod alignment within the core of the micelle has a large impact on the observed shapes and sizes of the micelle in selective solvents. These findings demonstrate that bond-bending potential is an effective and relatively simple parameter for modeling the chain rigidity of amphiphilic molecules. They also show that the modified DPD method is applicable for studying the self-assembly process of micelles from coil-rod-coil amphiphilic triblock copolymers.

## Acknowledgements

We thank the three anonymous referees whose critical comments helped us in improving the quality of our manuscript. We are grateful for the financial support provided by the Outstanding Youth Fund (No. 20525416) and the Program of the National Natural Science Foundation of China (Nos. 20874094 and 50773072), NBRPC (No. 2005CB623800) and SRFDP (No. 20810302058). X. Li acknowledges the financial support provided by China Postdoctoral Science Foundation (No. 20090460729). Parts of the simulations were carried out at the Shanghai Supercomputer Center (SSC).

## References and notes

1 P. Alexandridis and B. Lindman, *Amphiphilic Block Copolymers: Self-Assembly and Applications*, Elsevier, New York, 2000.
2 R. Zana, *Dynamics of Surfactant Self-Assemblies: Micelle, Microemulsions, Vescicles, and Lyotropic Phases*, CRC Press, Boca Raton, 2005.
3 K. Kataoka, A. Harada and Y. Nagasaki, *Adv. Drug Delivery Rev.*, 2001, **47**, 113–131.
4 D. J. Adams, S. Adams, D. Atkins, M. F. Butler and S. Furzeland, *J. Controlled Release*, 2008, **128**, 165–170.
5 L. Zhang and A. Eisenberg, *Science*, 1995, **268**, 1728–1731.
6 Y.-Y. Won, H. T. Davis and F. S. Bates, *Science*, 1999, **283**, 960–963.
7 S. Jain and F. S. Bates, *Science*, 2003, **300**, 460–464.
8 H. G. Cui, Z. Y. Chen, S. Zhong, K. L. Wooley and D. J. Pochan, *Science*, 2007, **317**, 647–650.
9 J. T. Chen, E. L. Thomas, C. K. Ober and S. S. Hwang, *Macromolecules*, 1995, **28**, 1688–1697.
10 J. T. Chen, E. L. Thomas, C. K. Ober and G.-P. Mao, *Science*, 1996, **273**, 343–346.
11 J. W. Park and E. L. Thomas, *Adv. Mater.*, 2003, **15**, 585–588.
12 J. W. Park and E. L. Thomas, *Macromolecules*, 2006, **39**, 4650–4653.
13 S. A. Jenekhe and X. L. Chen, *Science*, 1998, **279**, 1903–1907.
14 S. A. Jenekhe and X. L. Chen, *Science*, 1999, **283**, 372–375.
15 M. Mao and S. R. Turner, *J. Am. Chem. Soc.*, 2007, **129**, 3832–3833.
16 G. Gotzamanis and C. Tsitsilianis, *Macromol. Rapid Commun.*, 2006, **27**, 1757–1763.
17 H. Huo, K. Li, Q. Wang and C. Wu, *Macromolecules*, 2007, **40**, 6692–6698.
18 L. Huang, J. Hu, L. Lang, X. Zhang, X. Chen, Y. Wei and X. Jing, *Macromol. Rapid Commun.*, 2008, **29**, 1242–1247.
19 A. N. Semenov and S. V. Vasilenko, *Zh. Eksp. Teor. Fiz.*, 1986, **90**, 124–140.
20 D. R. M. Williams and G. H. Fredrickson, *Macromolecules*, 1992, **25**, 3561–3568.
21 R. Holyst and M. Schick, *J. Chem. Phys.*, 1992, **96**, 730–739.
22 M. Reenders and G. ten Brinke, *Macromolecules*, 2002, **35**, 3266–3280.
23 M. W. Matsen and C. Barrett, *J. Chem. Phys.*, 1998, **109**, 4108–4118.
24 V. Pryamitsyn and V. Ganesan, *J. Chem. Phys.*, 2004, **120**, 5824–5838.
25 W. Li and D. Gersappe, *Macromolecules*, 2001, **34**, 6783–6789.
26 J. Z. Chen, C. X. Zhang, Z. Y. Sun, Y. S. Zheng and L. J. An, *J. Chem. Phys.*, 2006, **124**, 104907.
27 J. Z. Chen, C. X. Zhang, Z. Y. Sun, L. J. An and Z. Tong, *J. Chem. Phys.*, 2007, **127**, 024105.
28 J. Z. Chen, Z. Y. Sun, C. X. Zhang, L. J. An and Z. Tong, *J. Chem. Phys.*, 2008, **128**, 074904.
29 Y. D. Xia, J. Z. Chen, Z. Y. Sun, T. F. Shi, L. J. An and Y. X. Jia, *J. Chem. Phys.*, 2009, **131**, 144905.
30 D. Düchs and D. E. Sullivan, *J. Phys.: Condens. Matter*, 2002, **14**, 12189–12202.
31 R. C. Hidalgo, D. E. Sullivan and J. Z. Y. Chen, *Phys. Rev. E: Stat., Nonlinear, Soft Matter Phys.*, 2005, **71**, 041804.
32 R. C. Hidalgo, D. E. Sullivan and J. Z. Y. Chen, *J. Phys.: Condens. Matter*, 2007, **19**, 376107.
33 K. H. Kim, J. Huh and W. H. Jo, *Macromolecules*, 2004, **37**, 676–679.
34 S. Lin, N. Numasawa, T. Nose and J. Lin, *Macromolecules*, 2007, **40**, 1684–1692.
35 C. R. Iacovella, M. A. Horsch and S. C. Glotzer, *J. Chem. Phys.*, 2008, **129**, 044902.
36 S. Lin, X. He, Y. Li, J. Lin and T. Nose, *J. Phys. Chem. B*, 2009, **113**, 13926–13934.
37 C. R. Iacovella and S. C. Glotzer, *Nano Lett.*, 2009, **9**, 1206–1211.
38 A. AlSunaidi, W. K. den Otter and J. H. R. Clarke, *J. Chem. Phys.*, 2009, **130**, 124910.
39 R. Diplock, D. E. Sullivan, K. M. Jaffer and S. B. Opps, *Phys. Rev. E: Stat., Nonlinear, Soft Matter Phys.*, 2004, **69**, 062701.
40 H. B. Movahed, R. C. Hidalgo and D. E. Sullivan, *Phys. Rev. E: Stat., Nonlinear, Soft Matter Phys.*, 2006, **73**, 032701.
41 Z. L. Zhang, M. A. Horsch, M. H. Lamm and S. C. Glotzer, *Nano Lett.*, 2003, **3**, 1341–1346.
42 M. A. Horsch, Z. L. Zhang and S. C. Glotzer, *Phys. Rev. Lett.*, 2005, **95**, 056105.
43 M. A. Horsch, Z. L. Zhang and C. S. Glotzer, *Nano Lett.*, 2006, **6**, 2406–2413.
44 T. D. Nguyen, Z. L. Zhang and S. C. Glotzer, *J. Chem. Phys.*, 2008, **129**, 244903.
45 T. D. Nguyen and S. C. Glotzer, *Small*, 2009, **5**, 2092–2098.
46 C. R. Iacovella and S. C. Glotzer, *Soft Matter*, 2009, **5**, 4492–4498.
47 J. H. Song, T. F. Shi, Y. Q. Li, J. Z. Chen and L. J. An, *J. Chem. Phys.*, 2008, **129**, 054906.
48 X. J. Li, M. G. Deng, Y. Liu and H. J. Liang, *J. Phys. Chem. B*, 2008, **112**, 14762–14765.
49 X. J. Li, P. T. He, D. Z. Kou, M. G. Deng and H. J. Liang. *J. Chem. Phys.*, submitted.
50 H. Noguchi and K. Yoshikawa, *J. Chem. Phys.*, 1998, **109**, 5070–5077.
51 N. Yoshinaga and K. Yoshikawa, *J. Chem. Phys.*, 2007, **127**, 044902.
52 J. C. Shillcock and R. Lipowsky, *J. Chem. Phys.*, 2002, **117**, 5048–5061.
53 M. Venturoli, B. Smit and M. M. Sperotto, *Biophys. J.*, 2005, **88**, 1778–1798.
54 H. J. Qian, L. J. Chen, Z. Y. Lu, Z. S. Li and C. C. Sun, *J. Chem. Phys.*, 2006, **124**, 014903.
55 H. J. Qian, L. J. Chen, Z. Y. Lu, Z. S. Li and C. C. Sun, *Europhys. Lett.*, 2006, **74**, 466–472.
56 L. Gao, J. Shillcock and R. Lipowsky, *J. Chem. Phys.*, 2007, **126**, 015101.
57 S. Yamamoto, Y. Maruyama and S. Hyodo, *J. Chem. Phys.*, 2002, **116**, 5842–5849.
58 S. Yamamoto and S. Hyodo, *J. Chem. Phys.*, 2003, **118**, 7937–7943.
59 M. Laradji and P. B. S. Kumar, *Phys. Rev. Lett.*, 2004, **93**, 198105.
60 M. Laradji and P. B. S. Kumar, *J. Chem. Phys.*, 2005, **123**, 224902.
61 H. B. Du, J. T. Zhu and W. Jiang, *J. Phys. Chem. B*, 2007, **111**, 1938–1945.
62 R. D. Groot and P. B. Warren, *J. Chem. Phys.*, 1997, **107**, 4423–4435.
63 G. De Fabritiis, M. Serrano, P. Español and P. V. Coveney, *Phys. A*, 2006, **361**, 429–440.
64 D. J. Pochan, Z. Y. Chen, H. G. Cui, K. Hales, K. Qi and K. L. Wooley, *Science*, 2004, **306**, 94–97.
65 X. H. He and F. Schmid, *Phys. Rev. Lett.*, 2008, **100**, 137802.
66 H. Z. Yu and W. Jiang, *Macromolecules*, 2009, **42**, 3399–3404.
67 J. Huh, W. H. Jo and G. ten Brinke, *Macromolecules*, 2002, **35**, 2413–2416.

 